$\mathcal{D}$-class of dark energy against ΛCDM in Brans-Dicke cosmology

A. Khodam-Mohammadi* and E. Karimkhani†

Department of Physics, Faculty of Science,

Bu-Ali Sina University, Hamedan 65178, Iran

Abstract

Three general models of dynamical interacting dark energy ($\mathcal{D}$-class) are investigated in the context of Brans-Dicke cosmology. All cosmological quantities such as equation of state parameters, deceleration parameters, Hubble function, and the density ratio are calculated as a function of redshift parameter. The most important part of this paper is fitting of models to the observational data (SNIa+BAO$_A$+Omh^2). We obtain a table of best fit value of parameters and report χ^2_{tot}/dof and Akaike Information Criterion (AIC) for each model. By these diagnostic tools, we find that some models have no chance against ΛCDM and some (e.g. $\mathcal{BD}-\mathcal{D}C2$ and $\mathcal{BD}-\mathcal{D}A^*$) render the best fit quality. Specially, the value of AIC analysis and figures show that the interacting $\mathcal{BD}-\mathcal{D}C2$ model fit perfectly with overall data and reveals a strong evidence in favor of this model, against ΛCDM.

* khodam@basu.ac.ir

† E.karimkhani91@basu.ac.ir

I. INTRODUCTION

The concordance model is one of the famous dark energy models (DE) that is supported by numerous observations that show an acceleration expansion of the universe such as subsequent measurements of distant supernova [1, 2] and most recently from the analysis of the precision cosmological data by the Planck collaboration [3]. In this model there exist a positive cosmological constant (CC) Λ term, so-called vacuum DE, which has been introduced first by Einstein and another terms that are contributed in the evolution of the universe such as matter (baryons plus cold dark matter) and radiation. Despite of good consistency with measurements, it suffers with two profound problem. One of them which is the most theoretical enigmas of fundamental physics, so-called cosmological constant problem [4, 5], or fine tuning, and the second one is Cosmic Coincidence problem (see e.g. the reviews [6–9]). The former namely the preposterous mismatch between the measured value from cosmological observations and the typical prediction for Λ in quantum field theory (QFT) [1–3] and the latter say about the ratio of dark matter to dark energy densities which must be bounded in order unity. It is a matter of fact that whether Λ or its density of energy ,$\rho_\Lambda = \Lambda/8\pi G$, is truly a constant or is a function of time (or scale factor $a(t)$ or Hubble rate $H(t)$). It is important to note that each model must satisfy at the same time theoretical considerations and constraints with observational data. Following this, different scenarios have been proposed. from one side, recently, a class of dynamical vacuum dark energy models (DVM's) were introduced [10] that Λ could be considered as a function of $\Lambda(H) = n_0 + n_1 H^2 + n_2 \dot{H} + ...$ [11] but equation of state is the same as CC (i.e. $w = P/\rho = -1$). In these models, authors have also considered an interaction between matter and dark energy in framework of the flat Friedmann-Lemaîter-Robertson-Walker (FLRW) in Einstein gravity and showed a "strong evidence" against the ΛCDM [12] , and hence in favor of the DVM's.

From the other side, many authors interested to consider dynamical dark energy models, with time varying $w(t)$, such as: scalar fields, both quintessence and phantom-like, modified gravity theories, phenomenological decaying vacuum models, holography scenarios, etc (cf. the previous review articles, references therein and [13, 14]). These models, can however alleviate the cosmological problems, specially cosmic coincidence problem, but they had done less investigation about the fine tuning problem. Hence, if we take the point of view that the dark energy density is a dynamical variable in quantum field theory in curved spacetime, it

will be possible to better tackle the basic CC problems, as well as the cosmic coincidence problem that may be solved by interacting dynamical DE models (e.g. see our previous paper [15]). Recently, one of us with some authors studied on the cosmological implications and linear structure formation of such dynamical dark energy, so-called $\mathcal{D}$-class. At last $\mathcal{D}$-models were fitted to the observational data and they showed that these models improve significantly the fit quality of the ΛCDM, showing that a moderate dynamical DE behavior is better than having a rigid Λ-term for the entire cosmic history [16].

Now we are in the point that using this kind of dynamical DE into the Brans-Dicke (BD) theory of gravity. For the reason that the $\mathcal{D}$-class DE density belongs to a dynamical cosmological constant, we need a dynamical framework to accommodate it instead of Einstein gravity. The best choice for this, is BD theory which is a scalar-tensor theory and was invented first by Jordan [17] and then ripened by brans and Dicke [18]. This theory is based on Mach's principle, which is a fundamental principle to explain the origin of inertia. In attempting to incorporate Mach's principle, the BD theory introduces a time dependent inertial scalar field φ, which plays the role of the gravitational constant G, so that $\varphi(t) \propto 1/G$ and is determined by distribution of mass of the universe . So the gravitational fields are described by the metric $g_{\mu\nu}$ and the BD scalar field φ, which has the dimension $[\varphi] = [M]^2$. In BD theory, the scalar field φ couples to gravity via a coupling parameter ω and it has been generalized for various scalar tensor theories. This theory passes the observational tests in the solar system domains [19] and also has been tested by some famous cosmological tests such as Cosmic Microwave Background (CMB) and Large Scale Structure (LSS) [20]. In recent years, many authors have been studied on the some models of DE (e.g. Holographic DE, Ricci DE, Ghost DE, and etc.) in the BD cosmology and have been found good result and fitting with observational data. Most of these models can fit in the category of general $\mathcal{D}$-class DE models. So this can be a good motivation for taking this class of DE models in the BD theory.

This paper is organized as follows. After a brief review on the Brans-Dicke cosmology, we introduce three classes of dynamical DE in Sec. II. The background solution and cosmological implications of each class of DE models are studied by different subsections in Sec III. The fitting of models to the observational data and make constraint of parameters of each model are performed in Sec. IV and at the following, in Sec. V, we give detailed discussion on the results by studying on the best fit quality and the chance of each model in

the competition of ΛCDM. Finally we finished our paper by some concluding and remarks.

II. GENERAL FORMALISM: DYNAMICAL DE IN THE FRAMEWORK OF BD COSMOLOGY

The BD action has been represented by

$$s = \int d^4x\sqrt{-g}\left(\phi R - \frac{\omega}{\phi}\partial_\mu\phi\partial^\mu\phi + \mathcal{L}_m\right), \tag{1}$$

where ϕ is Brans-Dicke scalar field, ω is the BD coupling parameter and $\mathcal{L}_m$ is the Lagrangian of matter. General relativity is a particular case of the BD theory, corresponding to $\omega \to \infty$ [21]. In a flat FRW universe, the BD field equations in a natural unit has been given as [22]

$$3H^2 - \frac{1}{2}\omega\frac{\dot{\phi}^2}{\phi^2} + 3H\frac{\dot{\phi}}{\phi} = \frac{1}{\phi}(\rho_m + \rho_D) \tag{2}$$

$$2\dot{H} + 3H^2 + \frac{1}{2}\omega\frac{\dot{\phi}^2}{\phi^2} + 2H\frac{\dot{\phi}}{\phi} + \frac{\ddot{\phi}}{\phi} = -\frac{1}{\phi}p_D, \tag{3}$$

where $H = \dot{a}/a$ is the Hubble function and the overdot denotes a derivative with respect to the cosmic time. At following, we are interested to consider that the total energy contents of our universe including a pressureless cold dark matter, a DE fluid which its dynamical equation of state (EoS) defines as $w_D = p_D/\rho_D$ and ignoring any radiation component.
As it is common in literatures, here we assume that the BD scalar field is proportional to the scale factor: $\phi = \phi_0 a^n = \phi_0(1+z)^{-n}$ where z is redshift and it is expected that n possess a tiny value in order to G changes by time slowly, which is consistent to our foundation about the universe. It is necessary to mention here that n will be considered as a free parameter and must be fitted with observational data. By inserting scale factor dependence of ϕ in Eqs. (2) and (3), we have

$$\rho_D = \frac{3\phi H^2\varsigma}{(1+u)}, \tag{4}$$

$$\rho_D = -\frac{H^2\phi}{w_D}\left(\frac{\dot{H}}{H^2}(2+n) + \vartheta\right). \tag{5}$$

where $\varsigma = 1 + n - \omega n^2/6$ and $\vartheta = 3 + 2n + n^2 + \omega n^2/2 = -3\varsigma + n^2 + 5n + 6$ are constants and $u = \rho_m/\rho_D$ define as the ratio of energy densities. As one may check in the limit $n = 0$, the Friedmann equations will be recovered. Let's remark that if we define the critical density

at present time as [1] $\rho_c^{(0)} = 3H_0^2\phi_0$, then following constraint could be satisfied by usage of Eq. (2) as

$$\Omega_m^{(0)} + \Omega_D^{(0)} + \Omega_\phi^{(0)} = 1. \tag{6}$$

Here $\Omega_\phi^{(0)} = \frac{1}{6}\omega n^2 - n$ and matter density parameter at present time take the following simple form

$$\Omega_m^{(0)} = \frac{u_0}{1+u_0}\varsigma, \tag{7}$$

where u_0 is the value of energy density ratio at present. At some points in next sections (III A, III B and III C) we will show that in order to determine the evolution of energy density versus redshift, $u(z)$, we need to fix u_0 and accordingly $\Omega_m^{(0)}$ parameters. But, as one may check from Eq. (7), these two parameters will be related to observation due to free parameter n which is hidden in ς quantity.

Considering Eqs. (4) and (5) we will gain a general equations which will be beneficial for our purpose in next sections. The equality of these two equations leads to following relation

$$\frac{\dot{H}}{H^2} = \frac{-3w_D\varsigma - \vartheta(1+u)}{(2+n)(1+u)} \tag{8}$$

The DE density and its dynamical nature plays a crucial role on the evolution of the universe. Hence, in the following we will consider three basic kind of dynamical DE models as

$$\begin{aligned}
\mathcal{BD}-\mathcal{D}A1: &\qquad \rho_D(H) = 3\phi\left(\alpha H^2 + \epsilon\right), \\
\mathcal{BD}-\mathcal{D}C1: &\qquad \rho_D(H) = 3\phi(\alpha H^2 + \beta H), \\
\mathcal{BD}-\mathcal{D}C2: &\qquad \rho_D(H) = 3\phi(\alpha H^2 + \gamma\dot{H})
\end{aligned} \tag{9}$$

where the "$\mathcal{BD}$" corresponds to Brans-Dicke cosmology and "$\mathcal{D}$" calls for dynamical nature of DE. Note that ϕ has dimension 2 (mass square) and two parameters α, γ are dimensionless but β, ϵ have dimension 1 and 2 in turn. Free parameters α and γ will be fitted by the observational data while β and ϵ could be restricted and related to the free parameters of each model which we will give a detailed discussion in next sections.

[1] One may defines $\rho_c^{(0)} = 3H_0^2\phi_0\varsigma$ and hence Eq. (7) reduced to $\Omega_m^{(0)} = \frac{u_0}{1+u_0}$ which is fixed for the present time with no dependence to free parameters of models that will be explained in Secs. III A, III B, III C and thus it is not preferred here.

III. COSMOLOGICAL BACKGROUND SOLUTION

In the following we will assume that the fluid contains two components, dark energy and dark matter, and to be more general we will regard two scenarios for these components:
†) Interacting case: These two components do not conserve separately but interact with each other in such a manner that the continuity equations take the form

$$\dot{\rho}_D + 3H(1 + w_D)\rho_D = -Q, \tag{10}$$

$$\dot{\rho}_m + 3H\rho_m = Q, \tag{11}$$

where Q stands for the interaction term. The ideal of interaction term must be motivated from the theory of quantum gravity but we my regard a pure dimensional basis for choosing an interaction Q. Usually in literature, the interaction term is defined in any of the following forms: (i) $Q \propto H\rho_D$, (ii) $Q \propto H\rho_m$, or (iii) $Q \propto H(\rho_m + \rho_D)$. Thus hereafter we choose only the first case, namely $Q = b^2 H\rho_D = \Gamma\rho_D$, where b^2 is a coupling constant and also we regard b^2 as a parameter to be fit with observational data.
‡) Non-interacting case: In this scenario dark matter and energy are considered self-conserved with no interaction with each other. Then for obtaining the corresponding equations in this case, it is enough to substitute $b^2 = 0$ in all gained equations of first scenario.
From Eqs. (10) and (11) one may derive an applicable equation for the evolution of the ratio of energy density as follows

$$\dot{u} = 3Hu\left[w_D + \frac{b^2}{3}\left(\frac{1+u}{u}\right)\right] \tag{12}$$

Equivalently, changing the cosmic time variable into the redshift due to relation $d/dt = -(1 + z)H(z)d/dz$, leads to

$$u'(z) = -\frac{3u(z)}{1+z}\left[w_D(z) + \frac{b^2}{3}\left(\frac{1+u(z)}{u(z)}\right)\right], \tag{13}$$

where prime denotes for derivative with respect to redshift. Also, for further analysis of background evolution of the universe, it will be beneficial to calculate deceleration parameter which defines as

$$q(z) = -1 - \frac{\dot{H}}{2H^2} = -1 + \frac{1+z}{2H^2(z)}\frac{dH^2(z)}{dz} \tag{14}$$

in which $H(z)$ will be calculated in each models.

A. $\mathcal{BD}-\mathcal{D}A1$ Model

We start with the calculation for the $\mathcal{BD}-\mathcal{D}A1$ model but before, it is worthwhile to mention here that, this model possesses a well-defined ΛCDM limit (i.e. $\rho = const$) for $\alpha = n = 0$. By the way in this model, using Eq.(4), the Hubble function can be gain as

$$H(t) = \pm\sqrt{\frac{-\epsilon(1+u(t))}{\alpha(1+u(t))-\varsigma}} \tag{15}$$

In the following, we will use Eq. (15) with minus sign. It will be feasible to gain constant ϵ in term of some other constants with solving eq. (15) at present time which will lead to

$$\epsilon = -H_0^2(\alpha - \frac{\varsigma}{1+u_0}). \tag{16}$$

Taking a derivation of Eq. (15) with respect to cosmic time we find

$$\frac{\dot{H}(t)}{H(t)^2} = \frac{\varsigma\dot{u}(t)}{2\sqrt{-\epsilon(\alpha(1+u(t))-\varsigma)(1+u(t))^3}}. \tag{17}$$

Using Eqs. (8) and (17) and taking into account that $d/dt = -(1+z)H(z)d/dz$, the EoS parameter can be given by

$$w_D(z) = -\frac{(1+z)(2+n)u'(z)}{6\,(\alpha(1+u(z))-\varsigma)} - \frac{\vartheta(1+u(z))}{3\varsigma}, \tag{18}$$

and substituting Eq. (13) in Eq. (18) gives

$$u'(z) = \frac{(1+u(z))}{1+z}\left[\frac{(\frac{\vartheta}{\varsigma}u(z)-b^2)}{1-\frac{(2+n)u(z)}{2(\alpha(1+u(z))-\varsigma)}}\right]. \tag{19}$$

By solving this equation, the redshift can be find versus u as follows

$$z = \left[\frac{\vartheta u - \varsigma b^2}{\vartheta u_0 - \varsigma b^2}\right]^{\frac{\varsigma(2\eta-\varsigma(n+2)b^2)}{2\eta(\vartheta+\varsigma b^2)}} \cdot \left[\frac{1+u}{1+u_0}\right]^{\frac{n-2\varsigma+2}{2(\varsigma b^2+\vartheta)}} \cdot \left[\frac{\alpha(1+u)-\varsigma}{\alpha(1+u_0)-\varsigma}\right]^{\frac{(2+n)(\varsigma-\alpha)}{2\eta}} - 1 \tag{20}$$

where

$$\eta = \vartheta(\alpha-\varsigma) + \alpha\varsigma b^2. \tag{21}$$

Finally the EoS parameter (18) and deceleration parameter (14), in term of energy density ratio by using of Eq. (19) can be rewritten as

$$w_D(z) = \left(\frac{1+u(z)}{3\varsigma}\right)\left[\frac{(2+n)b^2\varsigma - 2\vartheta(\alpha(1+u(z))-\varsigma)}{2(\alpha(1+u(z))-\varsigma)-(2+n)u(z)}\right] \tag{22}$$

$$q(z) = -1 - \frac{\vartheta u(z) - b^2\varsigma}{2(\alpha(1+u(z))-\varsigma)-(2+n)u(z)}. \tag{23}$$

As it is seen, the EoS and deceleration parameters do not depend on constant ϵ even by considering explicit formula of $u(z)$ versus z. This result is different with [16], where the same DE density was investigated in the framework of Hilbert-Einstein general relativity which was called $\mathcal{D}A1$ model there.

B. $\mathcal{BD}-\mathcal{D}C1$ Model

In this model, by using (4), the Hubble function is given by

$$H(t)=-\frac{\beta\,(1+u(t))}{\alpha\,(1+u(t))-\varsigma}. \tag{24}$$

By imposing the current value of Hubble function and energy density ratio in Eq. (24), One may fix the constant β as

$$\beta=-H_0\left(\alpha-\frac{\varsigma}{1+u_0}\right) \tag{25}$$

Using Eq. (24), we obtain

$$\frac{\dot{H}(t)}{H(t)^2}=\frac{\varsigma\dot{u}(t)}{\beta(1+u(t))^2} \tag{26}$$

and by equating this equation with (8), the EoS parameter can be written as

$$w_D(z)=-\frac{(1+z)(2+n)u'(z)}{3\,(\alpha(1+u(z))-\varsigma)}-\frac{\vartheta(1+u(z))}{3\varsigma} \tag{27}$$

As it is seen, β plays no role in the EoS parameter explicitly. Applying Eq. (13) in Eq. (27) leads to

$$u'(z)=\frac{(1+u(z))}{1+z}\left[\frac{(\frac{\vartheta}{\varsigma}u(z)-b^2)}{1-\frac{(2+n)u(z)}{\alpha(1+u(z))-\varsigma}}\right], \tag{28}$$

and solving above differential equation, (28), leads to an equation which shows the relation between redshift and energy density ratio in such a way that $u(z)$ is the root of following equation

$$z=\left[\frac{\vartheta u-\varsigma b^2}{\vartheta u_0-\varsigma b^2}\right]^{\frac{\varsigma(\eta-\varsigma(n+2)b^2)}{\eta(\vartheta+\varsigma b^2)}}\cdot\left[\frac{1+u}{1+u_0}\right]^{\frac{n-\varsigma+2}{(\varsigma b^2+\vartheta)}}\cdot\left[\frac{\alpha(1+u)-\varsigma}{\alpha(1+u_0)-\varsigma}\right]^{\frac{(2+n)(\varsigma-\alpha)}{\eta}}-1 \tag{29}$$

Finally, Eq. (28) help us to rewritten the EoS and deceleration parameters in term of energy density ratio as

$$w_D(z)=\left(\frac{1+u(z)}{3\varsigma}\right)\left[\frac{(2+n)b^2\varsigma-2\vartheta(\alpha(1+u(z))-\varsigma)}{\alpha(1+u(z))+\varsigma-(2+n)u(z)}\right] \tag{30}$$

and

$$q(z) = -1 + \frac{\vartheta u(z) - b^2\varsigma}{\varsigma + (2+n)u(z) - \alpha(1+u(z))}. \tag{31}$$

It must be mentioned that the non-interacting case is achieved by substituting $b^2 = 0$ in all above relations.

C. $\mathcal{BD} - \mathcal{DC}2$ Model

In previous sections, because of the form of DE density and by a straightforward approach we were able to gain an equation for Hubble function which depend on the energy density ratio. Here in this section we follow the procedure which is applied in ref. [15]. Substituting this form of DE density (from Eq. (9)) in Eq. (4), one can find

$$\frac{\dot{H}}{H^2} = \frac{\varsigma}{\gamma(1+u)} - \frac{\alpha}{\gamma} \tag{32}$$

Equating above equation with (8) gives a relation between EoS parameter and the energy density ration as follows

$$w_D = \frac{1}{3}\left[A(1+u(z)) - \frac{2+n}{\gamma}\right], \tag{33}$$

where

$$A = \frac{1}{\varsigma}\left[\frac{(2+n)\alpha}{\gamma} - \vartheta\right]. \tag{34}$$

The Deceleration parameter could also be calculated by using (32) as

$$q(z) = -1 + \frac{\alpha}{\gamma} - \frac{\varsigma}{(1+u(z))\gamma}. \tag{35}$$

Substituting Eq. (33) in (13), and then by solving the differential equation (13), we find

$$\begin{aligned} u(z) &= \frac{1}{2\gamma A}\Big\{C\tan\left[-\frac{C\ln(1+z)}{2\gamma} + \arctan\left(\frac{9\gamma A - 5n + 5\beta b^2 - 10)}{5C}\right)\right] \\ &\quad -\gamma A + 2 + n - \gamma b^2\Big\} \end{aligned} \tag{36}$$

where the parameter C is given by

$$C = \sqrt{4A\gamma(n+2) - (\gamma b^2 - 2 - A\gamma - n)^2}. \tag{37}$$

Using the continuity equation, (11), the density of dark matter in the interacting case yields

$$\rho_m = \rho_m^0(1+z)^3\exp[3b^2(\mathcal{F}(z) - \mathcal{F}(0))] \tag{38}$$

where

$$\mathcal{F}(z) = \frac{1}{2A}\times$$
$$\left\{ \ln(1+z)(A+b^2-\frac{1}{\gamma}) + \ln\left(1+\tan\left[-\frac{C\ln(1+z)}{2\gamma}+\arctan\left(\frac{9\gamma A-5n+5\gamma b^2-10)}{5C}\right)\right]^2\right)\right\} \tag{39}$$

and $\mathcal{F}(0)$ is the value of $\mathcal{F}(z)$ at present time. Also, ρ_m^0 could be obtain by using (4) as

$$\rho_m^0 = \frac{3\varsigma u_0 H_0^2\phi_0}{1+u_0} \tag{40}$$

At last, the Hubble function in terms of some known function of redshift can be given as follows

$$H(z) = \sqrt{\frac{\rho_m(z)}{3\varsigma\phi(z)}\left(\frac{(1+u(z))}{u(z)}\right)}. \tag{41}$$

IV. FITTING MODEL TO THE OBSERVATIONAL DATA

In this section in order to implement the fit, we interested to extract the combined data from expansion history: SNIa+BAO$_A$+Omh^2. Specifically in [23, 24] a very detailed description of all these cosmological observable is provided as well as of the fitting procedure, and the interested reader is refereed to these references for more information, see also [25, 26]. To get the best fit values of the relevant parameters, we maximize the likelihood function, $\mathcal{L} = e^{\chi^2{}_{tot}/2}$, or equivalently minimize the joint $\chi^2{}_{tot}$ function with respect to the elements (parameters) of $\mathbf{p}$ where

$$\chi^2_{tot}(\mathbf{p}) = \chi^2_{SNIa} + \chi^2_{BAO_a} + \chi^2_{omh^2}. \tag{42}$$

To compare the evidance for and against competing models it is common to employ various information creteria like Akaike Information Criterion (AIC) which in addition to χ^2, it takes into account the number of free parameters in each model, n_{fit}. Also it is appropriate for the models which we are studying here ($N_{tot}/n_{fit} > 40$) [27]. For the Gaussian errors it defines as:

$$AIC = \chi^2_{tot} + 2n_{fit} \tag{43}$$

The AIC grades two or more vying models and give in hand the numerical measure about each model which is preferred. In this way, AIC increment defines as $|\Delta(AIC)_{ij}|$ =

$|(AIC)_i - (AIC)_j|$, [16, 27]. Hence for a pairwise comparison, the conqueror model is one with smaller value of AIC. But it is needed to have $\Delta(AIC)_{ij} \geq 2$ because otherwise it betokens as consistency between these two model in competition, while for $\Delta(AIC)_{ij} \geq 6$ we will have a strong evidence for choosing preferred model. We will use this issues in next section.

Another point necessary to mention here is that in order to do constraint each model we have used $\omega = 1033$ which is gained form $PlanckTemp + PlanckLens$ at 99% confidence level under unrestricted supposition (no initial value for scalar field is fixed) [28] where it is consistent with what usually handled in literature: For example in [29] the authors has found $\omega \simeq 1000$ by using the CMB temperature and polarization anisotropy data, also see [30–32] and reference therein.

In the following we will explain each of SNIa, BAO$_A$ and Omh^2 analysis in short.

A. SNIa

First of all, we used the Union 2.1 set of 580 type Ia supernovae of Suzuki et al. [33]

$$\chi^2_{SNIa} = \sum_{i=1}^{580} \left[\frac{\mu_{th}(z_i,p) - \mu_{obs}(z_i)}{\sigma_i} \right]^2 \tag{44}$$

where z_i is the observed redshift for each data point. The observational modulus distance of SNIa, $\mu_{obs}(z_i)$, at redshift z_i is given by

$$\mu_{obs}(z_i) = m(z_i) - M \tag{45}$$

In theoretical point of view the modulus distance define as $\mu_{th}(z_i,p) = 5\log d_L + 25$, in which $d_L(z_i,p)$ is the luminosity distance for spatially flat universe:

$$d_L(z_i,p) = c(1+z) \int_0^z \frac{dz'}{H(z')}. \tag{46}$$

with c the speed of light. For doing the fit with SNIa data we have fixed H0 = 70 km/s/Mpc following the setting used in the Union 2.1 sample. σ_i defines as corresponding 1σ uncertainty for each SNIa data point.

It is worthy noting that in models with varying G, like BD theory, a correction must be regarded in order to employ the supernovae data. In [34, 35] who predicted on the basis of

an analytical model and reasonable assumptions that the SN Ia maximum luminosity can be expressed in terms of ejected nickel mass ($L \propto M_{Ni}$) which with a good approximation is a fixed fraction of the Chandrasekhar mass ($M_{Ni} \propto M_{Ch} \propto G^{-3/2}$) [36–38] and thus for the luminosity distance we will have $L \propto G^{-3/2}$. Using the definition of absolute magnitude

$$M = -2.5log\frac{L}{L_{\odot}} + cte, \tag{47}$$

the modulus distance relation must be corrected as [39]

$$\begin{aligned} \mu(z) &= \mu^{nc}_{obs} - \frac{15}{4}\log\frac{G}{G_0} \\ &= \mu^{nc}_{obs} + \frac{15}{4}\log\frac{\phi(z)}{\phi_0} = \mu^{nc}_{obs} - \frac{15}{4}n\log(1+z). \end{aligned} \tag{48}$$

in which we are using $\phi \propto a^n$ in the third relation and quantity μ^{nc}_{obs} is the observed distant modulus before correction.

B. BAO$_A$

The BAO estimators A(z) collected by Blake et al. in [40]. The BAO measurement at the largest redshift H(z = 2.34) taken after [41] on the basis of BAO's in the Lyα forest of BOSS DR11 quasars. The acoustic parameter, A(z), for BAO introduced by Eisenstein as follows [42]:

$$A(z_i, p) = \frac{\sqrt{\Omega^{(0)}_m}}{E(z_i)^{\frac{1}{3}}}\left[\frac{1}{z_i}\int_0^{z_i}\frac{dz}{E(z)}\right]^{\frac{2}{3}} \tag{49}$$

Where $E(z) = H(z)/H_0$ and z_i is the redshift at which this observable is measured. For BAO_A we have used the current value of the Hubble function given by the Planck Collaboration [3], i.e. $H0 = 67.8km/s/Mpc$. The corresponding χ^2-functions for BAO_A analysis are defined as:

$$\chi^2_{BAO_A} = \sum_{i=1}^{6}\left[\frac{A_{th}(z_i, p) - A_{obs}(z_i)}{\sigma_{A,i}}\right]^2 \tag{50}$$

where the corresponding values for z_i, A_{obs} and $\sigma_{A,i}$ can be found in table 3 of [40].

C. Omh^2

We use the available measurements of the Hubble function as collected in [43]. These are essentially the data points of [44] in the redshift range $0 \leqslant z \leqslant 1.75$ and we define the

Model	α	$\Omega_m^{(0)}/\gamma$	b^2	n	χ^2/dof	AIC
ΛCDM	-	0.275 ± 0.005	-	-	808.083/991	810.083
$\mathcal{BD}-\mathcal{D}A1$	0.331 ± 0.022	-	$0.373^{+0.020}_{-0.009}$	0.009 ± 0.025	801.531/989	807.531
$\mathcal{BD}-\mathcal{D}$C1 $(\alpha:-)$	$-0.300^{+0.011}_{-0.001}$	-	$0.287^{+0.048}_{-0.034}$	0.020 ± 0.002	800.076/989	806.076
$\mathcal{BD}-\mathcal{D}$C1 $(\alpha:+)$	0.044 ± 0.016	-	$0.441^{+0.026}_{-0.008}$	0.018 ± 0.001	807.144/989	813.144
$\mathcal{BD}-\mathcal{D}$C2	$0.765^{+0.027}_{-0.003}$	$0.430^{+0.008}_{-0.020}$	$0.051^{+0.018}_{-0.004}$	$-0.009^{+0.014}_{-0.006}$	791.735/988	799.735
$\mathcal{BD}-\mathcal{D}A1^\star$	$-0.073^{+0.003}_{-0.001}$	-	-	$0.014^{+0.001}_{-0.002}$	793.485/990	797.485
$\mathcal{BD}-\mathcal{D}C1^\star$	$-0.315^{+0.003}_{-0.006}$	-	-	$0.006^{+0.006}_{-0.001}$	815.210/990	817.210
$\mathcal{BD}-\mathcal{D}C2^\star$	$0.976^{+0.003}_{-0.051}$	$0.614^{+0.040}_{-0.012}$	-	$-0.019^{+0.001}_{-0.007}$	831.811/989	837.811

TABLE I: The best-fitting values for the various models and their statistical significance (χ^2-test and Akaike information criterion, AIC, see Sect. IV) for both interacting and non-interacting (indicated by $\star$) cases. All quantities corresponds to the expansion history of universe i.e. (BAO$_A$+SNIa+Omh^2). The given values in third column is correspond to $\Omega_m^{(0)}$ (resp. γ) for ΛCDM (resp. $\mathcal{BD}-\mathcal{D}C2$) model. Details of the fitting observables are given in Sect. IV.

following $\chi^2_{Omh^2}$ function, to be minimized:

$$\chi^2_{Omh^2} = \sum_{i=1}^{N-1} \sum_{j=i+1}^{N} \left[\frac{Omh^2_{th}(H_i, H_j) - Omh^2_{obs}(H_i, H_j)}{\sigma_{Omh^2\, i,j}} \right]^2 , \tag{51}$$

where N is the number of points $H(z)$ contained in the data set, $H_i \equiv H(z_i)$, and $Omh^2(H_i, H_j)$ is the two-point diagnostic [45],

$$Omh^2(z_2, z_1) \equiv \frac{h^2(z_2) - h^2(z_1)}{(1+z_2)^3 - (1+z_1)^3}, \tag{52}$$

with $h(z)/h \equiv H(z)/H_0$, and $\sigma_{Omh^2\, i,j}$ is the uncertainty associated to the observed value $Omh^2_{obs}(H_i, H_j)$ for a given pair of points ij, viz.

$$\sigma^2_{Omh^2\, i,j} = \frac{4\left[h^2(z_i)\sigma^2_{h(z_i)} + h^2(z_j)\sigma^2_{h(z_j)}\right]}{\left[(1+z_i)^3 - (1+z_j)^3\right]^2} . \tag{53}$$

In [23], [24] a more detailed explanation of all these cosmological observables as well as on the fitting procedure has been elaborated, and therefore we have left more details aside from the present work.

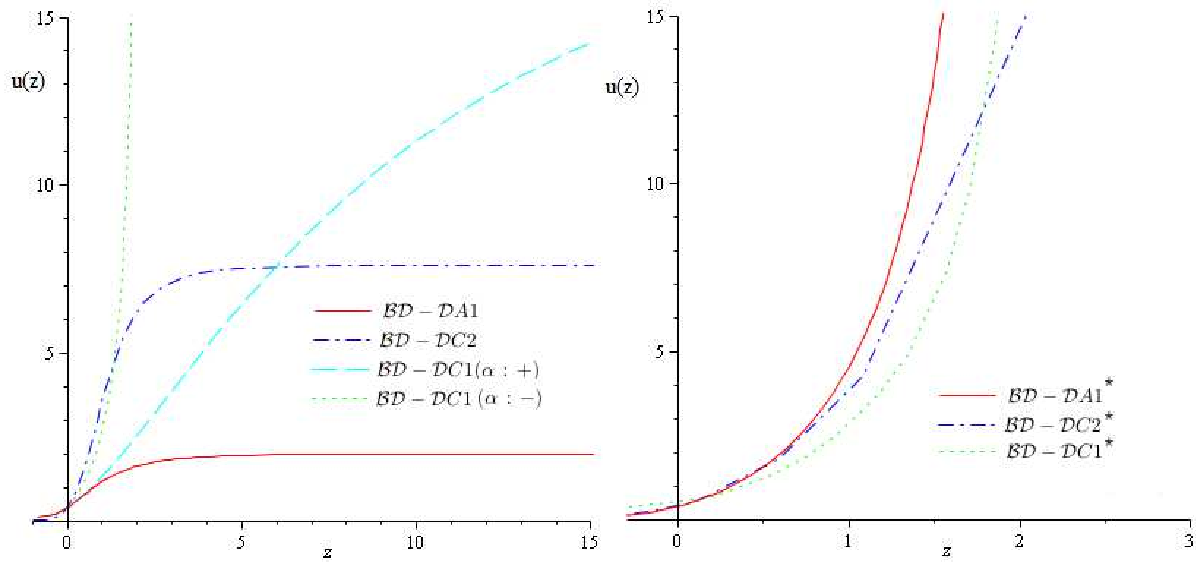

FIG. 1: Energy density ratio versus redshift for interacting (left) and non-interacting (right) models under consideration. In all plots we have used the best fit values of Table 1

V. DISCUSSION AND RESULTS

In this section we provide further discussion on the results and the calculations which has been done in previous sections. The plots for EoS, deceleration parameters and energy density ratio will be illustrate here. At the end we will see which model place in the more prominent position in competing with the others and has the most harmony with observation.

In table I, the best fitted values of parameters of each mentioned models, using the discussed statistical analysis, have been collected. These values are used for studying of other cosmological parameters in the bulk. In this table χ^2_{tot}/dof has been reported where dof is number of degrees of freedom and define as: $dof = N_{tot} - n_{fit}$ in which N_{tot} is the number of data points and n_{fit} is the model-dependent number of fitted parameters.

In Fig. 1 the energy density ratio as a function of cosmic redshift for both interacting (left) and non-interacting (right) has been plotted by using Eqs. (20), (29) and (36). This evolutionary illustration is significant from the point of view of investigation of coincidence problem. As it is seen in Fig. 1, the energy density ratio for $\mathcal{BD}-\mathcal{D}A1$, $\mathcal{BD}-\mathcal{D}C1(\alpha:+)$ and $\mathcal{BD}-\mathcal{D}C2$ models has been bounded in the past and future which could be alleviate the coincidence problem. Whilst for all non-interacting models and also $\mathcal{BD}-\mathcal{D}C2(\alpha:-)$

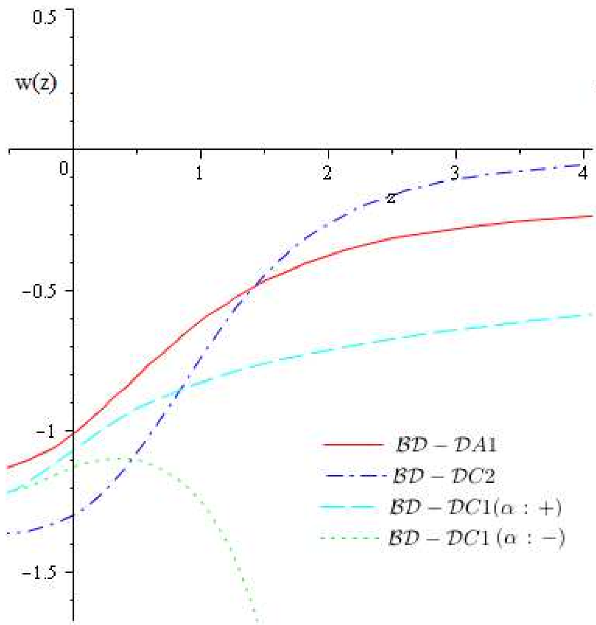

FIG. 2: EoS function, $\omega_D(z)$, versus cosmic redshift for interacting (left) and non-interacting (right) models using the best fit values of Table. I.

no bound is seen. We find that in all models for $\alpha < 0$, the coincidence problem can not be solved.

Considering Eqs. (22), (30) and (33) the behavior of EoS versus redshift is depicted in Fig. 2. Also, substituting the best-fit values of the parameters, according to the results shown in table I, in the mentioned formula the current value of the EoS parameter achieved for $\mathcal{BD}-\mathcal{DA}1$ Model reads $w_D^{(0)} = -1.005$. This result is perfectly compatible with current observational evidence from Planck result where $w_D^{(0)} = -1.006 \pm 0.045$ [3]. While for non-interacting case, $\mathcal{BD}-\mathcal{DA}1^{\star}$, it reads as $w_D^{(0)} = -1.086$ and furthermore an asymptotic behavior is seen in its plot (right) for $z \approx 2$.

The point worthwhile to add here is that in [16] the same DE density is studied on the background of general relativity and on the Assumption of non-interacting model, where it is called $\mathcal{DA}1$ model. There, asymptotic behavior is seen for $\mathcal{DA}1$ model (Fig. 2 of [16]). So by collating this with obtained results here we may state that interaction plays a crucial role for elimination of asymptotic behavior.

For both of $\mathcal{BD}-\mathcal{DC}1$ sub-classes, the EoS parameter exhibit a phantom like behavior but as it is seen in Fig. 2, the subclass with $(\alpha:-)$ display a vertical asymptote at high redshift $(z > 1.5)$. Using the best fitted values for free parameters of $\mathcal{BD}-\mathcal{DC}1:(\alpha:-),(\alpha:+)$

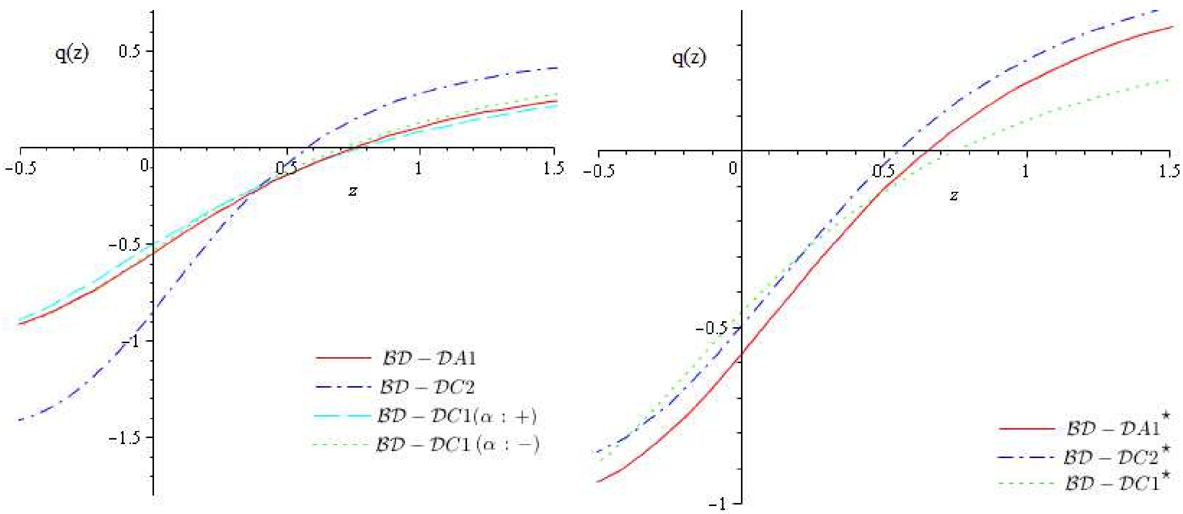

FIG. 3: Deceleration parameter, $q(z)$, and transition point from deceleration to acceleration for interacting (left) and non-interacting (right) models.

leads to $w_D^{(0)} = -1.127$ and $w_D^{(0)} = -1.062$ in turn. Incidentally, for $\mathcal{BD}-\mathcal{D}C1^{\star}$ we have $w_D^{(0)} = -0.909$ which is far from observational results. Hence, as it explained before, the sub-class with $(\alpha : +)$ exhibits value much closer to current value of EoS parameter at present, according to observation [3].

Using the best fitted values for free parameter of $\mathcal{BD}-\mathcal{D}C2$ (resp. $\mathcal{BD}-\mathcal{D}C2^{\star}$) model, the EoS parameter at present time gains as $w_D^{(0)} = -1.296$ (resp. $w_D^{(0)} = -1.075$) which indicates that the interacting $\mathcal{BD}-\mathcal{D}C2$ possess the much larger negative values between all other models.

The evolution of deceleration parameter, by using Eqs. (23), (31) and (35), is illustrated in Fig. 3 . As one can check from Fig. 3, all model has a deflection point in the past where the accelerating universe transit from deceleration to acceleration. Finding the root of $q(z)$ function, the point Z_{tr} in all models can be given. According to best fit values in table I, deceleration parameter and redshift transition point for $\mathcal{D}$-class models are given in table II. As one can see from table II, similar to EoS parameter, in $\mathcal{BD}-\mathcal{D}C2$ model, the present value of q is larger (in absolute value) than the other models.

Now we will focus on Fig. 4, where the 2-dimensional plots for the physical region of parameters of $\mathcal{BD}-\mathcal{D}C2$ model has been depicted. The corresponding plots for the

	$\mathcal{BD}-\mathcal{D}A1$	$\mathcal{BD}-\mathcal{D}A1^{\star}$	$\mathcal{BD}-\mathcal{D}C1$ $(\alpha:+)$	$\mathcal{BD}-\mathcal{D}C1$ $(\alpha:-)$	$\mathcal{BD}-\mathcal{D}C1^{\star}$	$\mathcal{BD}-\mathcal{D}C2$
$q^{(0)}$	-0.543	-0.579	-0.498	-0.529	-0.460	-0.844
z_{tr}	0.745	0.650	0.780	0.708	0.750	0.573

TABLE II: Present deceleration parameter and redshift transition point for $\mathcal{D}$-class models.

other models is somewhat similar and not shown here. The $\mathcal{BD}-\mathcal{D}C2$ model depiction is presented here because of the most parameter it possesses and for this depiction we have utilized the expansion history data (Omh^2+BAO_A+SNIa). The bounds with elliptically shapes corresponds with 1σ, 2σ and 3σ confidence levels. In order to appraise the statistical analyze quality and do the comparison between different models studied in this work, the χ^2 and AIC values have displayed in table I. A glance at this table reveals that the fit quality for all models except $\mathcal{BD}-\mathcal{D}C1^{\star}$, $\mathcal{BD}-\mathcal{D}C2^{\star}$ and $\mathcal{BD}-\mathcal{D}C1(\alpha:+)$ are better than ΛCDM model. Meanwhile among all these models, the $\mathcal{BD}-\mathcal{D}C2$ and $\mathcal{BD}-\mathcal{D}A1^{\star}$ render the best fit quality (the smallest value of χ^2/dof among all others).

As explained in Sec. IV using AIC increment, we are able to compare interacting and non interacting i=$\mathcal{BD}-\mathcal{D}A1$, $\mathcal{BD}-\mathcal{D}C1$ and $\mathcal{BD}-\mathcal{D}C2$ models with the j=ΛCDM. Hence, from table I for interacting $\mathcal{BD}-\mathcal{D}A1$ model (resp. non-interacting one) we find $|\Delta(AIC)| \geq 2$ (resp. $|\Delta(AIC)| \geq 12$) against ΛCDM. So notice that as it is seen from the upshot of AIC increment, evidence for non-interacting case is more stronger than the interacting one. However as we mentioned previously, in $\mathcal{BD}-\mathcal{D}A1^{\star}$ model, the problem of cosmic coincidence has remained and this model could be ruled out.

Now it is turn to investigate $\mathcal{BD}-\mathcal{D}C1$ model but as we will see this model has no enough chance in the competition with ΛCDM. For $\mathcal{BD}-\mathcal{D}C1(\alpha:-)$ we have $|\Delta(AIC)| \geq 4$ against ΛCDM while for $\mathcal{BD}-\mathcal{D}C1(\alpha:+)$ and $\mathcal{BD}-\mathcal{D}C1^{\star}$ we have in turn $|\Delta(AIC)| \geq 3$ and $|\Delta(AIC)| \geq 7$ against these models.

Therefor we are face with strong evidence against $\mathcal{BD}-\mathcal{D}C1^{\star}$ and also outcomes from background history investigation reveals phenomenologically problematic issues(coincidence problem and inconsistency with current observational data) for this model. So due to these obstacles, this model does not possess the ability for proper adjustment with expansion

history of universe and could be ruled out.

About the $\mathcal{BD}-\mathcal{D}C1(\alpha:+)$ model, as it is explained in previous section this model is introduced here because of alleviation of coincidence problem (according to Fig. 1), but the AIC increment manifests it does not present statistically adequate result versus ΛCDM. On the other hand $\mathcal{BD}-\mathcal{D}C1(\alpha:-)$ model is exactly in opposite point of the $\mathcal{BD}-\mathcal{D}C1(\alpha:+)$, i.e. it suffers from cosmic coincidence problem but shows better AIC analysis.

Finally, we assess the viability of $\mathcal{BD}-\mathcal{D}C2$ model. AIC increment for interacting $\mathcal{BD}-\mathcal{D}C2$ model (resp. $\mathcal{BD}-\mathcal{D}C2^{\star}$) reads as $|\Delta(AIC)| \geq 10$ (resp. $|\Delta(AIC)| \geq 27$) against ΛCDM which of course are strong evidence in favor of (or against) these models.

Hence, according to Fig 1, 2 and 3 and also AIC analysis, the $\mathcal{BD}-\mathcal{D}C2$ model fit perfectly with overall data and in physical point of view.

VI. CONCLUSIONS

Three models of $\mathcal{D}$-class of interacting and non-interacting dark energy, investigated in the context of Brans-Dike theory of gravity. The Hubble parameter, equation of state and deceleration parameters were given and showed that the cosmic coincidence problem may be alleviated in some parameters ($\alpha > 0$) and almost in interacting cases. After fitting parameters of each model with observational data (SNIa+BAO$_A$+Omh^2) and compare with ΛCDM model, we found following facts:

1. In $\mathcal{BD}-\mathcal{D}A1$ model, the cosmic coincidence is alleviated only for interacting case and the equation of state in present time has a good consistency with plank result ($w_D^{(0)} = -1.005$). The value of AIC is near the AIC of ΛCDM ($3 > |\Delta(AIC)| > 2$) and this model may be (week) favored against ΛCDM. Also its minimum χ^2/dof is smaller than ones of ΛCDM.

2. In $\mathcal{BD}-\mathcal{D}C1$ model as the previous case, the cosmic coincidence is only alleviated for interacting and ($\alpha > 0$) case. In this case its AIC is bigger than AIC of ΛCDM which is reveal a not-favored model against ΛCDM.

3. In $\mathcal{BD}-\mathcal{D}C2$ model, the cosmic coincidence alleviated for interacting and $\alpha > 0$ case since the absolute value of $|\Delta(AIC)| \geq 10$. This fact reveals a strong evidence in favor of this model against ΛCDM model.

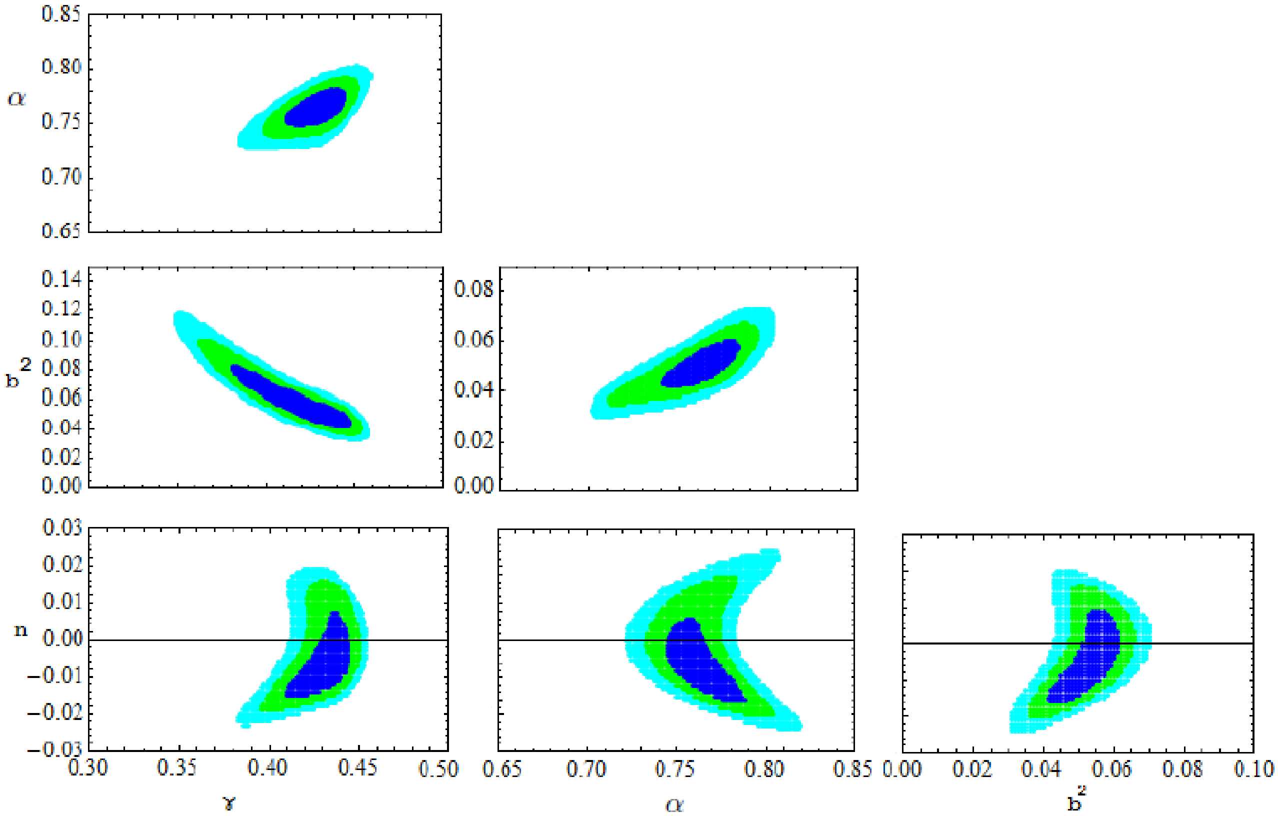

FIG. 4: 2-dimensional Likelihood contours of the cosmological and model parameters (for the values $-2\ln\mathcal{L}/\mathcal{L}_{max} = 2.30,\ 6.16, 11.81$, corresponding to 1σ, 2σ and 3σ confidence levels) for the $\mathcal{BD}-\mathcal{DC}2$ model using the full expansion history: (Omh^2+BAO_A+SNIa) data.

Finally, we expect that this facts may also be confirmed after studying on the structure formation of these models, specially $\mathcal{BD}-\mathcal{DC}2$. We leave it into the future works.

Acknowledgments

We would like to express sincere gratitude to Joan Solà for constructive comments and discussion. E. Karimkhani would also like to thank Adrià Gómez-Valent for sharing his knowledge on data fitting procedure.

---

[1] S. Perlmutter et al. [Supernova Cosmology Project Collaboration], Astrophys. J. **517** (1999) 565.

[2] A. G. Riess et al. [Supernova Search Team Collaboration], Astron. J. **116** (1998) 1009.

[3] P.A.R Ade et al. [Planck Collaboration], *Planck 2015 results. XIII. Cosmological parameters*, accepted by Astronomy and Astrophysics (2016) [arXiv:1502.01589].

[4] J. Solà, J. Phys. Conf. Ser. **453** (2013) 012015. [arXiv:1306.1527].

[5] J. Solà, Int. J. Mod. Phys. D**24** (2015) 1544027.

[6] E.J Copeland, M. Sami, & S. Tsujikawa, Int. J. Mod. Phys. D**15** (2006) 1753.

[7] T. Padmanabhan, Phys. Rep. **380** (2003) 235.

[8] P.J.E. Peebles, and B. Ratra, Rev. Mod. Phys. **75** (2003) 559.

[9] J. Solà, *Cosmological constant and vacuum energy: old and new ideas*, J. Phys. Conf. Ser. **453** (2013) 012015 [arXiv:1306.1527].

[10] J. Solà, A. Gómez-Valent, Int. J. Mod. Phys. D**24** (2015) 1541003 [arXiv:1501.03832].

[11] J. Solà [arXiv:1601.01668].

[12] J. Solà, Javier de Cruz Perez, Adria Gomez-Valent, Rafael C. Nunes [arXiv:1606.00450].

[13] E. J. Copeland, M. Sami, and S. Tsujikawa, Int. J. Mod. Phys., D**15** (2006) 1753.

[14] M. Li, X.-D. Li, S. Wang, and Y. Wang, Commun. Theor. Phys., **56** (2011) 525.

[15] A. Khodam-Mohammadi, E.Karimkhani, A.Sheykhi, Int.J.Mod. Phys.D, **23** (2014) 14500813.

[16] A. Gómez-Valent, E. Karimkhani, J. Solà, JCAP **12** (2015) 048.

[17] P. Jordan, Schwerkraft and Waltall (Friedrich Vieweg und Sohn, Braunschwig), Nature **164**, 637 (1955).

[18] C. Brans, and R.H. Dicke, Phys. Rev. **124**, 925 (1961); R. H. Dicke, Phys. Rev. **125** (1962) 2163.

[19] B. Bertotti, L. Iess, and P. Tortora, Nature, **425** (2003) 374.

[20] Xuelei Chen and Marc Kamionkowski, Phys.Rev. D**60** (1999) 104036; V. Acquaviva and L. Verde, JCAP, **0712** (2007) 001; S. Tsujikawa, K. Uddin, S. Mizuno, R. Tavakol, and J. Yok oyama, Phys.Rev. D**77** (2008) 103009; F. Wu and X. Chen, Phys.Rev. D**82** (2010) 083003; F. Wu and X. Chen, Phys.Rev. D**88** (2013) 084053.

[21] S. Weinberg, Rev. Mod. Phys. **61** (1989) 1.

[22] N. Banerjee, and D., Pavon, Class. Quant. Grav. **18** (2001) 593.

[23] A. Gómez-Valent, J. Solà and S. Basilakos, JCAP **01** (2015) 004.

[24] A. Gómez-Valent and J. Solà, Mon. Not. Roy. Astron. Soc. **448** (2015) 2810.

[25] S. Basilakos, M. Plionis and J. Solà, Phys. Rev. D**80** (2009) 3511.

[26] J. Grande, J. Solà, S. Basilakos, and M. Plionis, JCAP **1108** (2011) 007.

[27] H. Akaike, IEEE Transactions of Automatic Control, **19** (1974) 716; N. Sugiura, Communications in Statistics A, Theory and Methods, **7** (1978) 13; K.P. Burnham and D.R. Anderson, *Model selection and multimodel inference* (Springer, New York, 2002).

[28] A. Avilez and C. Skordis, Phys. Rev. Lett. **113** (2014) 011101.

[29] X.-l. Chen and M. Kamionkowski, Phys.Rev., **D60** (1999) 104036.

[30] V. Acquaviva and L. Verde, JCAP, **0712** (2007) 001.

[31] Ji-Xia Li et al Res. Astron. Astrophys. **15** (2015) 2151.

[32] H. Alavirad and A. Sheykhi, Phys. Lett. B., **734** (2014) 148.

[33] N. Suzuki et al, Astrophys. J. **746** (2012) 85.

[34] W.D. Arnett, Astrophysical Journal **254** (1982) 1.

[35] W.D. Arnett, Astrophysical Journal, **253** (1982) 785.

[36] A. Khokhlov, E. Muller and P. Höflich, A&A, **270**, (1993) 223.

[37] Jordi Gomez-Gomar, Jordi Isern, and Pierre Jean , MNRAS, **295** (1998) 1.

[38] D. Branch, to appear in Young Supernova Remnants, ed.: S.S. Holt and U. Hwang, New York: AIP (2001), [astro-ph/0012300].

[39] Ji-Xia Li et al., Research in Astron. and Astophys., **15** (2015) 2151.

[40] C. Blake et al., Mon. Not. Roy. Astron. Soc., **418** (2011) 1707.

[41] Delubac, T., et al., A&A **574** (2015) A59.

[42] D. J. Eisenstein et al. (SDSS Collab.), Astrophys. J. **633** (2005) 560 [astro-ph/0501171].

[43] X. Ding et al., Astrophys. J. **803** (2015) L22 [arXiv:1503.04923].

[44] O. Farooq, B. Ratra, Astrophys. J. **766** (2013) L7.

[45] V. Sahni, A. Shafieloo and A. A. Starobinsky, Astrophys. J. **793** (2014) L40 [arXiv:1406.2209].